IAI Journals.ASM.org

# Control of Mycobacterial Infections in Mice Expressing Human Tumor Necrosis Factor (TNF) but Not Mouse TNF

Maria L. Olleros,[a] Leslie Chavez-Galan,[a,j] Noria Segueni,[b] Marie L. Bourigault,[b] Dominique Vesin,[a] Andrey A. Kruglov,[c,d,e] Marina S. Drutskaya,[f] Ruth Bisig,[a] Stefan Ehlers,[g] Sahar Aly,[g]* Kerstin Walter,[h] Dmitry V. Kuprash,[e,f] Miliana Chouchkova,[i] Sergei V. Kozlov,[k] François Erard,[b] Bernard Ryffel,[b] Valérie F. J. Quesniaux,[b] Sergei A. Nedospasov,[c,d,e,f] Irene Garcia[a]

Department of Pathology and Immunology, CMU, Faculty of Medicine, University of Geneva, Geneva, Switzerland[a]; University of Orleans and CNRS, UMR7355, and Experimental and Molecular Immunology and Neurogenetics, Orleans, France[b]; Belozersky Institute of Physico-Chemical Biology and Biological Faculty, Lomonosov Moscow State University, Moscow, Russia[c]; German Rheumatism Research Center (DRFZ), a Leibniz Institute, Berlin, Germany[d]; Laboratory of Experimental Immunology, Lobachevsky State University of Nizhni Novgorod, Nizhni Novgorod, Russia[e]; Engelhardt Institute of Molecular Biology, Russian Academy of Sciences, Moscow, Russia[f]; Priority Research Area Infections, Research Center Borstel, Borstel, Germany[g]; German Center for Infection Research, Thematic Translational Unit Tuberculosis, Braunschweig, Germany[h]; BulBio-National Center of Infectious and Parasitic Diseases, Sofia, Bulgaria[i]; Laboratory of Integrative Immunology, National Institute of Respiratory Diseases, Mexico City, Mexico[j]; Center for Advanced Preclinical Research, Laboratory Animal Sciences Program, Leidos Biomed, Inc., Frederick, Maryland, USA[k]

**Tumor necrosis factor (TNF) is an important cytokine for host defense against pathogens but is also associated with the development of human immunopathologies. TNF blockade effectively ameliorates many chronic inflammatory conditions but compromises host immunity to tuberculosis. The search for novel, more specific human TNF blockers requires the development of a reliable animal model. We used a novel mouse model with complete replacement of the mouse TNF gene by its human ortholog (human TNF [huTNF] knock-in [KI] mice) to determine resistance to *Mycobacterium bovis* BCG and *M. tuberculosis* infections and to investigate whether TNF inhibitors in clinical use reduce host immunity. Our results show that macrophages from huTNF KI mice responded to BCG and lipopolysaccharide similarly to wild-type macrophages by NF-κB activation and cytokine production. While TNF-deficient mice rapidly succumbed to mycobacterial infection, huTNF KI mice survived, controlling the bacterial burden and activating bactericidal mechanisms. Administration of TNF-neutralizing biologics disrupted the control of mycobacterial infection in huTNF KI mice, leading to an increased bacterial burden and hyperinflammation. Thus, our findings demonstrate that human TNF can functionally replace murine TNF *in vivo*, providing mycobacterial resistance that could be compromised by TNF neutralization. This new animal model will be helpful for the testing of specific biologics neutralizing human TNF.**

Tumor necrosis factor (TNF) is critical for resistance against intracellular bacterial infections; however, its dysregulation may be associated with the development of human immunopathologies (1–5). Anti-TNF therapies have shown their efficacy for the treatment of autoimmune inflammatory diseases, such as rheumatoid arthritis and Crohn's disease, and are being explored for the treatment of other severe human pathologies, such as chronic obstructive pulmonary disease (6–8). However, the complete blockade of TNF has confirmed the essential role of TNF in the control of tuberculosis (TB) infection, as treated patients develop both TB and nontuberculous mycobacterial diseases (9–12). TB is still a major health problem newly affecting in its active form nearly 9 million people every year. One-third of the global population is considered to be infected by *Mycobacterium tuberculosis* in a latent form (13). *M. bovis* BCG is used for vaccination in countries with a high TB incidence and appears to control severe forms of tuberculosis in children but fails to prevent TB in adults (14).

TNF is initially synthesized as a membrane protein released under activation by infectious and inflammatory stimuli. Two types of TNF inhibitors blocking membrane and soluble TNF are currently used to treat inflammatory diseases and comprise anti-TNF antibodies (infliximab, adalimumab, certolizumab, etc.) and soluble TNF receptor 2 (sTNFR2; etanercept) (15). These drugs have distinct neutralization efficacies in human diseases, and they are associated with distinct risks of TB reactivation, with the anti-TNF antibody-based drugs showing more pronounced TB reactivation than sTNFR2 (16, 17). However, mechanistically this phenomenon is not well understood and cannot be studied in mouse models since the antibodies are species specific and only biologics that are based on the TNF receptor and that react with mouse TNF can be tested *in vivo* (15, 18). To that end, Plessner et al. compared soluble murine TNFR2-Fc to an anti-mouse TNF antibody and reported that while during primary infection both TNF inhibitors had similar effects of exacerbating TB infection, the effect of sTNFR2 during chronic infection was less than that of the antibody due to decreased penetration into granulomas (19). Never-

Received 5 June 2015 Accepted 24 June 2015

Accepted manuscript posted online 29 June 2015

Citation Olleros ML, Chavez-Galan L, Segueni N, Bourigault ML, Vesin D, Kruglov AA, Drutskaya MS, Bisig R, Ehlers S, Aly S, Walter K, Kuprash DV, Chouchkova M, Kozlov SV, Erard F, Ryffel B, Quesniaux VFJ, Nedospasov SA, Garcia I. 2015. Control of mycobacterial infections in mice expressing human tumor necrosis factor (TNF) but not mouse TNF. Infect Immun 83:3612–3623. doi:10.1128/IAI.00743-15.

Editor: S. Ehrt

Address correspondence to Irene Garcia, Irene.garcia-gabay@unige.ch.

* Present address: Sahar Aly, Charité, University Medicine Berlin, Medical Clinic for Infection Biology and Pneumology, Berlin, Germany.

Supplemental material for this article may be found at http://dx.doi.org/10.1128/IAI.00743-15.



doi:10.1128/IAI.00743-15

theless, most TNF blockers are human specific and do not interact with mouse TNF, creating one of the limitations to their *in vivo* analysis. To test new molecules inhibiting human TNF *in vivo* and select the best candidates, a specific mouse model is required. In the present study, mice with human TNF, in which the mouse TNF gene was replaced by the human TNF gene (human TNF [huTNF] knock-in [KI] mice), were used to show that human TNF expressed in mice can functionally substitute for mouse TNF in terms of the development of host immunity in response to mycobacterial infections. We further demonstrate that anti-human TNF antibodies used in the clinic jeopardize such protection, validating the use of this animal model for testing the effects of new human-specific TNF-neutralizing molecules.

## MATERIALS AND METHODS

**Ethics statement.** Animal experiments were approved by the Cantonal Veterinary Office of Geneva, Switzerland (authorization no. 31.1.1005/3202/2), the Ethics Committee for Animal Experimentation of CNRS Campus Orleans (authorization no. CLE CCO 2012-1001), and the Ministry of Environment, Nature Protection and Agriculture in Kiel, Germany (authorization no. V312-72241.1123-3(36-3/09).

**Mice.** Mice with human TNF (huTNF KI) were generated by the conventional technology of homologous recombination in embryonic stem cells, followed by removal of the positive selection marker using a LoxP-Cre system. The mouse genomic locus containing the TNF gene was replaced by the syntenic portion of the human genome (see Fig. S1 in the supplemental material), resulting in full replacement of mouse TNF by its human ortholog (20) (A. A. Kruglov, I. A. Mufazalov, A. A. Kuchmiy, M. S. Drutskaya, and S. A. Nedospasov, unpublished data). C57BL/6, huTNF KI, and TNF knockout (KO) (21) mice were housed under conventional conditions at CMU and under specific-pathogen-free conditions at CNRS (TAAM UPS44, Orleans, France) and the Research Center Borstel (RCB).

**BMDM culture.** Bone marrow-derived macrophages (BMDMs) were derived from bone marrow cells obtained from femurs and cultured as described previously (22). BMDMs were infected with BCG Connaught (multiplicity of infection [MOI], 1) or activated with lipopolysaccharide (LPS; 1 μg/ml; *Escherichia coli* serotype O111:B4; Sigma) or with gamma interferon (IFN-γ; 100 units/ml), and supernatants were harvested after 24 h.

**Evaluation of cytokines, chemokines, and TNF bioactivity.** Cytokines (TNF, IFN-γ, interleukin-12 p40 [IL-12p40]) and chemokines (RANTES, monocyte chemoattractant protein 1 [MCP-1]) in cellular supernatants, serum, and lung tissues (homogenized in 0.04% Tween 80, NaCl, 125 mg tissue per ml) were evaluated by enzyme-linked immunosorbent assay. The TNF bioactivity of BMDM culture supernatants was measured on WEHI164 cells (subclone 13) as described previously (23). Addition of sTNFR1 (5 μg/ml) from sTNFR1-transgenic mouse serum (24) or anti-TNF (2 μg/ml; MP6-XT22) inhibited the TNF bioactivity of the samples.

**BCG and *M. tuberculosis* infections and treatment with TNF blockers.** Mice were infected intravenously (i.v.) with $5 \times 10^6$ CFU of living BCG strain Sofia (25), $1 \times 10^7$ CFU of living BCG strain Connaught (26), or $5 \times 10^6$ CFU of BCG Pasteur strain 1173 P2, as indicated below. Survival experiments were pursued for up to 200 days. Intraperitoneal injection of infliximab (10 mg/kg of body weight; Remicade; Centocor) or vehicle (0.9% NaCl) was performed at day 6 postinfection and twice a week for 3 weeks. Mice were infected either intranasally (i.n.) with 1,000 CFU or by aerosol infection with 500 CFU of *M. tuberculosis* H37Rv using a Glas-Col aerosol infection device (Terre-Haute, IN). TNF blockers were diluted in 0.9% NaCl, and intraperitoneal application started at day 14 postinfection and was continued for 2 weeks. Infliximab (Remicade) and adalimumab (Humira) were administered once a week (10 mg/kg), while the treatment with etanercept (Enbrel) was done twice weekly (40 mg/kg). Lung bacterial load and pathology were determined at the time points postinfection indicated below (27–29).

**Histological analyses, ZN staining, and acid phosphatase activity.** Histological analyses of infected organs were done at 4 weeks postinfection on fixed tissues for hematoxylin and eosin (H&E) and Ziehl-Neelsen (ZN) staining and on frozen livers for determination of acid phosphatase activity (24). Histopathological analyses were performed on tissue sections from lung and liver using digital microscopic images acquired by a Mirax digital slide scanner and analyzed with Pannoramic Viewer software (Carl Zeiss) (30). For liver analysis, the area with lesions was quantified and is presented as the percentage of the area with lesions, corresponding to the area of granulomas/surface area of the total liver, which was $50 \pm 11$ mm$^2$ per liver section and animal. For lung analysis, the areas without and with lesions were quantified in a lung surface area of $40 \pm 18$ mm$^2$ per lung section (one or two lobes) and per animal. Data are presented as the percentage of the free alveolar space, corresponding to the percentage of the area lung lesion free/total area of lung. Cellular infiltration, necrosis, and edema were quantified using a semiquantitative score indicating the increasing severity of changes (range of scores, 0 to 5). The scoring was performed by two independent observers, including a trained pathologist.

**Western blot analyses.** Liver proteins were analyzed by Western blotting as described previously (31). The primary antibody was either a rabbit polyclonal anti-NF-κB p65 antibody (Santa Cruz Biotech) or a rabbit monoclonal anti-phosphorylated NF-κB p65 antibody (Cell Signaling Tech), and the secondary antibody was a horseradish peroxidase-conjugated goat anti-rabbit antibody (Bio-Rad). We used a polyclonal rabbit anti-mouse inducible nitric oxide synthase (iNOS; Calbiochem) and an antiactin antibody (Sigma-Aldrich). Blots were developed with LumiGlo chemiluminescent substrate (KPL). The density of the bands was quantified by Quantity One analysis software (Bio-Rad).

***Ex vivo* stimulation and flow cytometry analyses of splenocytes.** Spleen cells from mice that had been infected for 4 weeks ($5 \times 10^6$ CFU of BCG Pasteur) were prepared as described previously (32). Splenocytes were stimulated with medium, BCG culture filtrate antigens (CFAs; 20 μg/ml), and BCG (MOI, 1), and supernatants were evaluated for IFN-γ and nitric oxide (NO). Nitrite content, as an indicator of the NO content, was assessed by use of the Griess reagent (31).

Flow cytometry on splenocytes was performed using a FACSCyan flow cytometer (Beckman Coulter, Inc.), and 50,000 events were typically acquired. The following antibodies were used: anti-CD3 (145-2C11), anti-CD4 (GK1.5), anti-Ly6G (RB6-8C5), anti-major histocompatibility complex class II (anti-MHC-II; M5/114.15.2), and anti-CD11b (M1/70) from eBioscience (San Diego, CA) and 2.4G2 anti-Fcγ RII/III monoclonal antibody. Data were analyzed with FlowJo software (Tree Star, Inc., Ashland, OR). To precisely control the gating, appropriate fluorochrome-labeled isotype control antibodies were used and fluorescence minus 1 was used as a control.

**Statistical analyses.** Statistical analyses were done with GraphPad Prism software (GraphPad Soft., La Jolla, CA). A $P$ value of $<0.05$ was considered statistically significant. Data from experiments with 2 groups were analyzed with an unpaired Student $t$ test, and data from experiments with more than two groups were analyzed with one-way analysis of variance (ANOVA) and nonparametric Turkey tests.

## RESULTS

**Cytokine responses and NF-κB activation in BMDMs from huTNF KI mice.** To determine whether macrophages from huTNF KI mice (see Fig. S1 in the supplemental material) have the capacity to respond normally to BCG infection and to other stimuli, bone marrow-derived macrophages (BMDMs) from huTNF KI mice were compared to wild-type (WT) cells for their ability to produce cytokines. The levels of murine TNF induced by BCG, LPS, and IFN-γ in WT BMDMs were similar to those of human TNF activated in huTNF KI BMDMs (Fig. 1A). No measurable

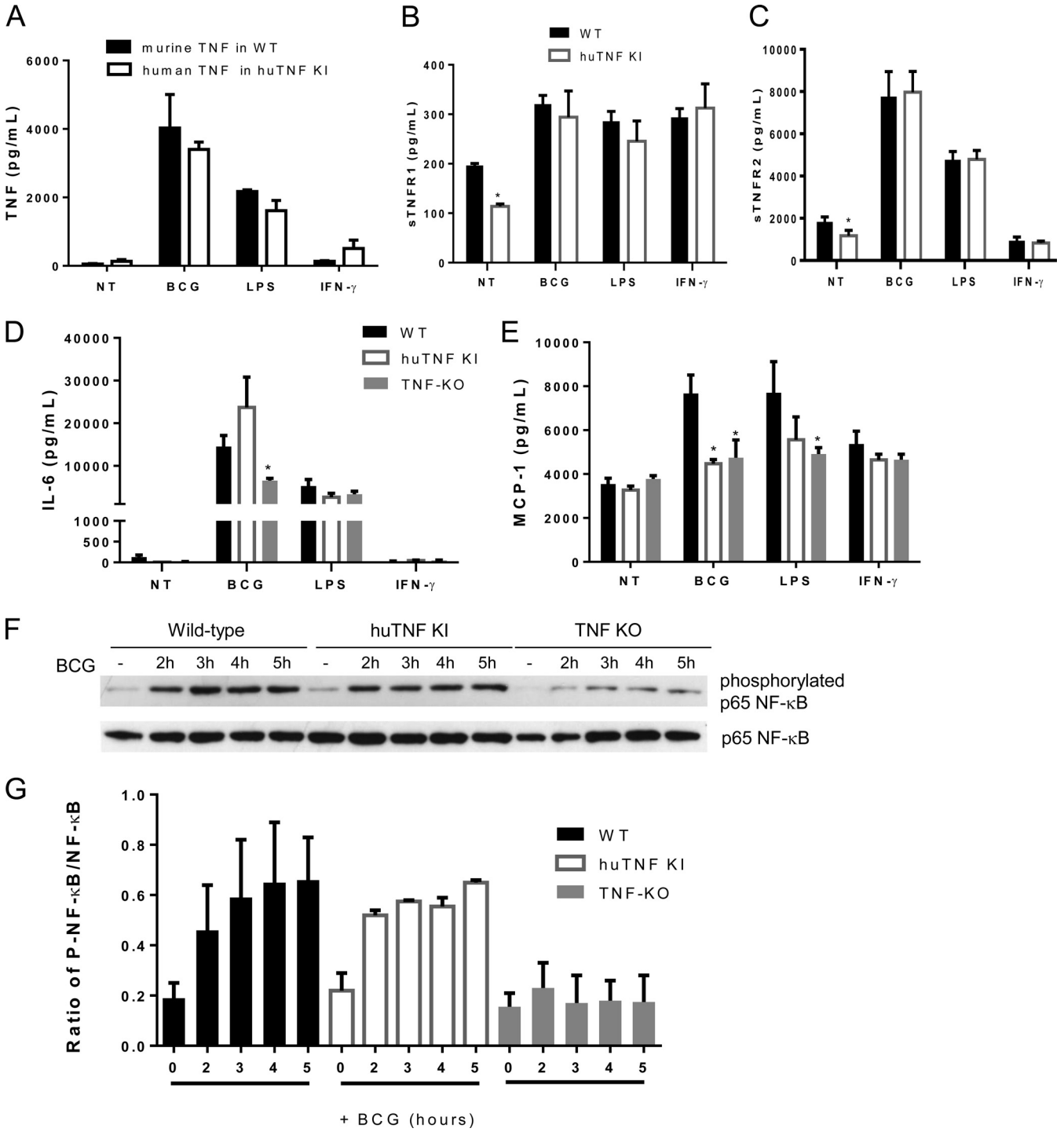


**FIG 1** BMDMs from huTNF KI mice respond to BCG, LPS, and IFN-γ as well as WT cells producing cytokines, chemokines, and phosphorylated NF-κB p65 upon BCG infection. BMDMs from huTNF KI and WT mice were activated for 24 h with BCG Connaught (MOI, 1), LPS, or IFN-γ. (A) Murine TNF concentrations in the supernatants of WT BMDMs and human TNF concentrations in the supernatants of huTNF KI BMDMs. (B to E) The levels of soluble TNFR1 (B), soluble TNFR2 (C), IL-6 (D), and MCP-1 (E) in culture supernatants were determined ($n = 6$). NT, not treated. (F) Phosphorylated and nonphosphorylated NF-κB p65 proteins in BMDMs uninfected or infected with BCG were detected by Western blotting at different time points. One of three representative Western blots is shown. (G) The graph presents the ratio of phosphorylated NF-κB p65 (P-NF-κB) to nonphosphorylated NF-κB p65 bands from three Western blots corresponding to three experiments. Quantification was done with Quantity One analysis software, and results are presented as the ratio of the number of units of phosphorylated NF-κB p65/number of units of total NF-κB p65 ($n = 3$ mice per group). The bar graphs show means ± SEMs. *, $P < 0.05$ versus the WT.

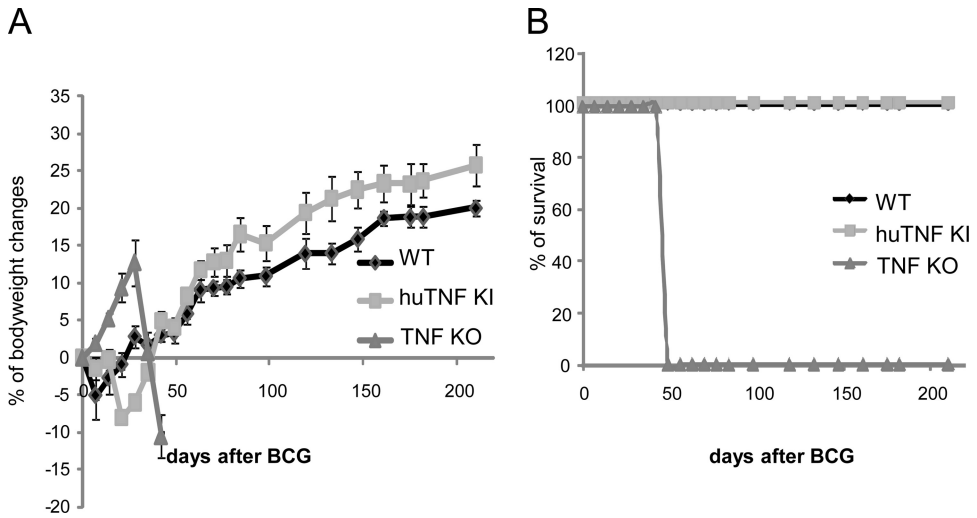


**FIG 2** huTNF KI mice survive BCG infection as well as WT mice. (A) Body weight changes after infection of WT, huTNF KI, and TNF KO mice with BCG Connaught ($10 \times 10^6$ CFU). (B) The survival of BCG-infected mice was monitored for more than 200 days postinfection ($n = 7$ for WT mice, $n = 9$ for huTNF KI mice, $n = 3$ for TNF KO mice).

human TNF was released by activated WT murine cells and vice versa, indicating that all assays were species specific (data not shown). The levels of bioactive TNF made by BCG-infected BMDMs were similar in huTNF KI and WT cell supernatants, as measured by WEHI164 cell death induction (see Fig. S2A in the supplemental material). The concentrations of activated soluble TNFR1 and TNFR2 in both WT and huTNF KI BMDM supernatants were comparable (Fig. 1B and C). IL-6 levels were similar in huTNF KI and WT BMDMs, while BCG-infected TNF KO BMDMs produced smaller amounts of IL-6 (Fig. 1D). Interestingly, the level of BCG-induced MCP-1 expression by huTNF KI BMDMs was significantly lower than that by WT cells (Fig. 1E). To assess whether BMDMs from huTNF KI mice can activate intracellular signaling after BCG infection, NF-κB phosphorylation patterns were analyzed by Western blotting. The levels of phosphorylated NF-κB p65 progressively increased in WT and huTNF KI BMDMs after BCG infection, and both WT and huTNF KI BMDMs presented a similar activation profile, which appeared to be much lower in TNF KO BMDMs than in WT BMDMs (Fig. 1F and G; see also Fig. S2B in the supplemental material). Human TNF in huTNF KI macrophages lacking endogenous mouse TNF expression was efficiently induced by different stimuli, including live mycobacteria.

**HuTNF KI mice are resistant to BCG infection.** The previous results encouraged us to explore the ability of human TNF to protect mice from BCG infection *in vivo*. Infection of huTNF KI, TNF KO, and WT mice with BCG (Connaught, $1 \times 10^7$ CFU) led to a dramatic loss of body weight and the rapid death of TNF KO mice, while both huTNF KI and WT mice resisted the infection for more than 6 months of the experiment (Fig. 2A and B). Similar results were obtained after infection with the BCG Pasteur strain ($5 \times 10^6$ CFU), with huTNF KI mice surviving for over 4 months (not shown). We then infected mice with the attenuated BCG Sofia strain ($5 \times 10^6$ CFU) (25), and TNF KO mice survived for more than 8 weeks after infection. Liver and lung bacterial loads were highly increased in TNF KO mice at 8 weeks after infection but were less increased in huTNF KI mice, which harbored intermediate bacterial loads compared with those harbored by WT mice (Fig. 3A and B). Histopathologic examination revealed that the liver granulomas of huTNF KI mice were transiently of a smaller size but later appeared to be well differentiated and similar to those observed in WT mice, correlating with the acid phosphatase activity which is expressed by activated monocytes/macrophages, including epithelioid cells recruited to liver granulomas, as previously described (33). Granulomas were not formed in the liver of TNF KO mice infected for 4 weeks, in which only a weak acid phosphatase activity of Kupffer cells was observed, and after 8 weeks, the granulomas were very small and had impaired acid phosphatase activity (Fig. 3C). Similarly, at 4 weeks of infection, the number of hepatic granulomas was transiently lower in huTNF KI mice than in WT mice and hepatic granulomas were absent in TNF KO mice. After 8 weeks of infection, similar numbers were observed in both huTNF KI and WT mice but very low numbers were observed in TNF KO mice (Fig. 3D). A similar pattern was obtained after analysis of the liver area with lesions (see Fig. S3A in the supplemental material). We also explored the development of bactericidal mechanisms, such as iNOS activation, a mechanism essential for BCG clearance and mouse survival (34). The level of expression of iNOS in huTNF KI and TNF KO mice correlated with the number of liver granulomas, and at 8 weeks postinfection, it was found that the livers from huTNF KI mice but not those from TNF KO mice expressed functional granulomas, as did the livers of WT mice (Fig. 3E and F). These data indicate that although huTNF KI mice may have a delay in BCG-induced immune responses, these mice are able to activate bactericidal mechanisms and control the infection.

**Human TNF expression sustains BCG induction of cytokines and chemokines.** To explore whether huTNF KI mice respond to BCG infection by producing Th1-type cytokines and chemokines like WT mice do, the levels of IFN-γ, IL-12p40, RANTES, and MCP-1 in the lungs during BCG infection were evaluated. The lung IFN-γ, IL-12p40, RANTES, and MCP-1 levels of huTNF KI mice were similar to those of WT mice, but the levels were lower in the lungs of TNF KO mice (Fig. 4A to D). Serum cytokine and chemokine levels showed more variation in huTNF

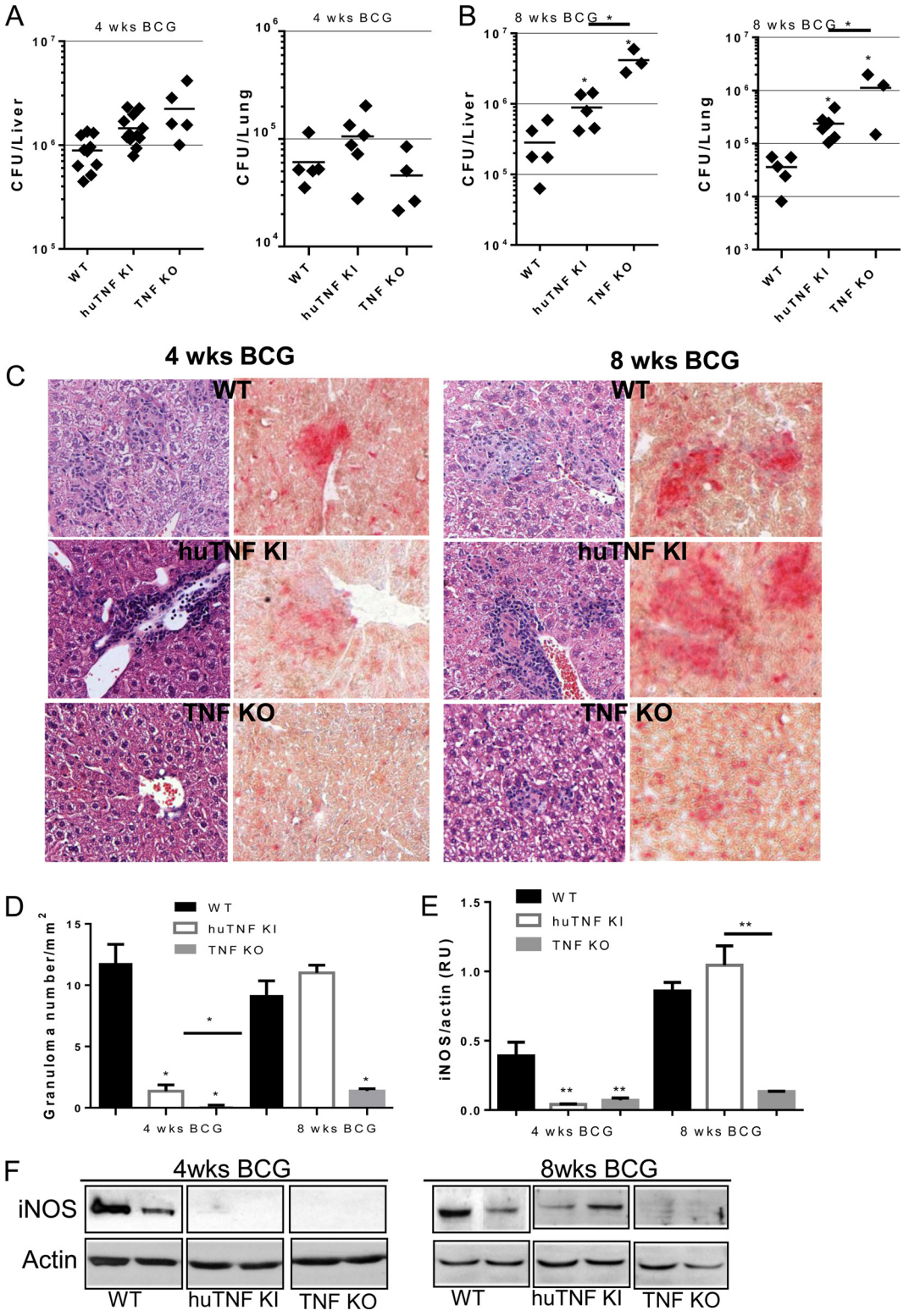


**FIG 3** Bacterial load, granuloma formation, and iNOS expression in huTNF KI mice during BCG infection. (A and B) Liver and lung bacterial loads in WT, huTNF KI, and TNF KO mice at 4 weeks (A) and 8 weeks (B) after BCG infection ($5 \times 10^6$ CFU of BCG Sofia strain) ($n = 9$ for WT and huTNF KI mice, $n = 4$ for TNF KO mice). (C) Microscopic examination of liver granulomas in WT, huTNF KI, and TNF KO mice after H&E staining (left) and acid phosphatase activity (right) on liver sections at 4 and 8 weeks after infection. The liver sections show the granulomas in WT mice in comparison with the granulomas in huTNF KI mice but absence in TNF KO mice correlating with the acid phosphatase activity of active monocytes/macrophages forming granulomas (activity is colored in red). The images are representative of those from two experiments ($n = 6$ to 7 per group). Magnifications, ×400. (D) The number of liver granulomas in WT, huTNF KI, and TNF KO mice was assessed at 4 and 8 weeks postinfection ($n = 6$ for WT mice, $n = 10$ for huTNF KI mice, $n = 3$ for TNF KO mice). (E) Level of hepatic iNOS protein expression relative to the level of actin expression at 4 and 8 weeks after BCG infection on Western blots. Protein expression was determined with Quantity One analysis software in three different experiments. RU, relative units. (F) Representative Western blot revealing iNOS and actin ($n = 8$ for WT and huTNF KI mice, $n = 3$ for TNF KO mice). Bar graphs show means ± SEMs. *, $P < 0.05$ versus WT mice; **, $P < 0.01$ versus WT mice.

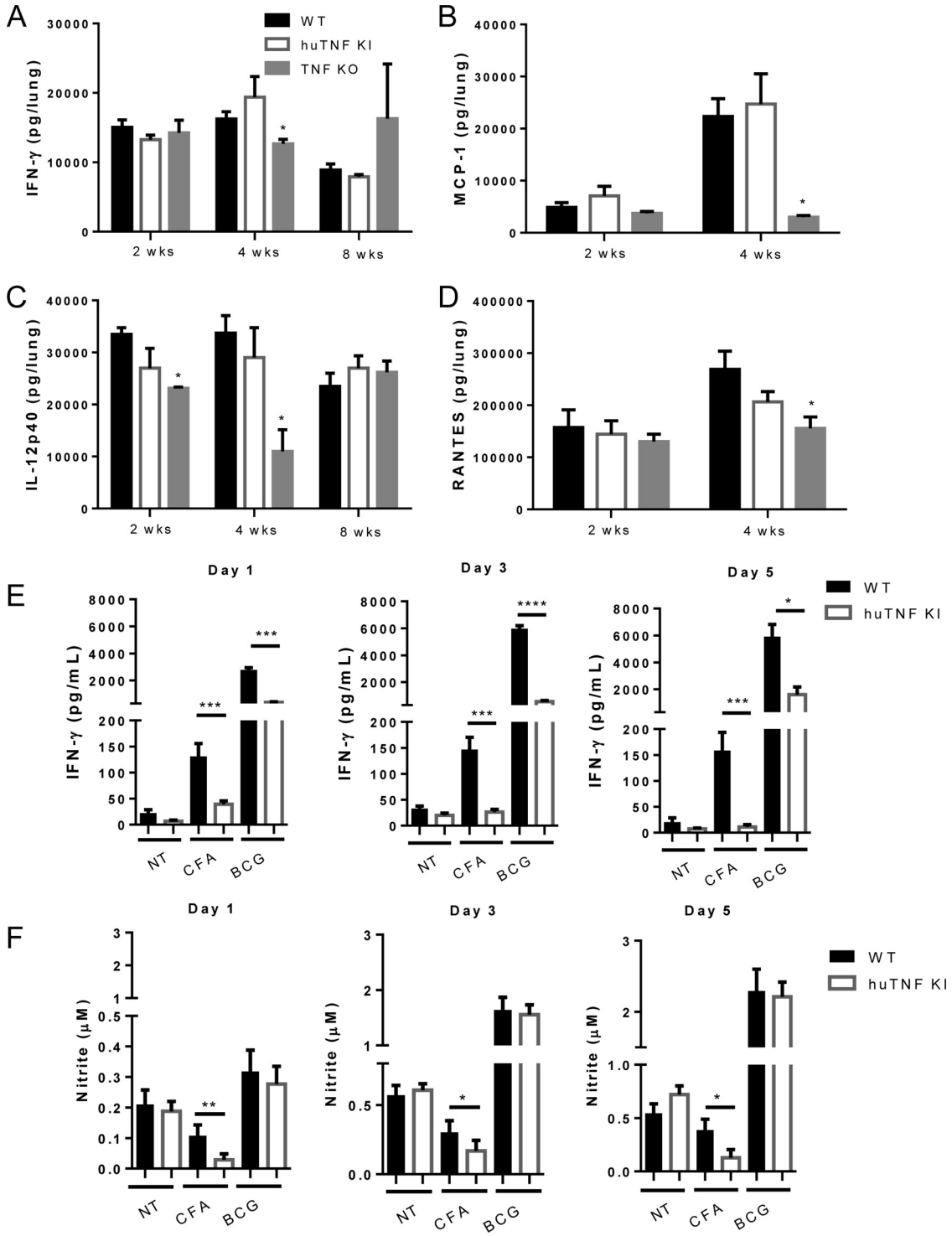


**FIG 4** Pulmonary levels of cytokines and chemokines during BCG infection and after *ex vivo* splenocyte stimulation. (A to D) Lung IFN-γ (A), IL-12p40 (B), RANTES (C), and MCP-1 (D) levels in WT, huTNF KI, and TNF KO mice ($n = 4$ to 9 per group) were assessed at the indicated time points postinfection. (E and F) IFN-γ (E) and nitrite (F) levels in culture supernatants of splenocytes derived from mice infected with BCG for 4 weeks after incubation with culture filtrate antigens (CFAs; 20 μg/ml) or BCG Pasteur (MOI, 1) ($n = 4$ animals per group) were evaluated. Bar graphs show means ± SEMs. *, $P < 0.05$ versus WT mice; **, $P < 0.01$ versus WT mice; ***, $P < 0.001$ versus WT mice; ****, $P < 0.0001$ versus WT mice. NT, not treated.

KI mice than WT mice at early times after infection, but at late time points they were similar in these two groups of mice, which is in contrast to the dysregulation observed in TNF KO mice (see Fig. S2A to D in the supplemental material). Thus, the expression of human TNF in huTNF KI mice allowed the expression of IFN-γ, IL-12p40, RANTES, and MCP-1 in response to BCG infection, which was impaired in TNF KO mice.

We further analyzed the capacity of lymphocytes from huTNF

KI mice infected with BCG to respond to antigenic stimulation by production of IFN-γ. Restimulation of splenocytes with CFA and BCG resulted in lower levels of IFN-γ in huTNF KI splenocytes than in WT cells at 4 weeks postinfection (Fig. 4E). Nitrite levels were also decreased in huTNF KI splenocytes after CFA activation, while BCG infection led to similar NO amounts, suggesting that the huTNF KI macrophage function was similar to that of WT cells (Fig. 4F). We asked if IFN-γ production by huTNF KI splenocytes could be attributed to differences in the number of splenic $CD3^+/CD4^+$ T cells at this time point. Fluorescence-activated cell sorter analyses showed that the $CD3^+$ $CD4^+$ T cell population was lower in huTNF KI mice than WT mice but that the total numbers of $CD11b^+$ Ly6G-positive cells (neutrophils) and $CD11b^+$ MHC-II-positive cells (macrophages) were comparable in huTNF KI and WT mice at 4 weeks postinfection (see Fig. S4 in the supplemental material).

**HuTNF KI mice become sensitive to BCG infection upon treatment with infliximab.** Inhibition of mouse TNF by anti-mouse TNF antibodies during BCG infection has demonstrated the critical role of TNF during this infection (24, 35). Therefore, in the present study, we evaluated whether inhibition of human TNF in huTNF KI mice may render animals susceptible to mycobacterial infection. Anti-human TNF administration to mice at day 6 postinfection and then twice a week for 3 weeks postinfection did not affect WT mice but clearly resulted in increased bacterial loads in both the spleens and lungs of huTNF KI mice at 4 weeks postinfection (Fig. 5A and B). Relative lung weight, as a first indicator of lung inflammation, was increased in infliximab-treated huTNF KI mice but not in vehicle-treated controls (Fig. 5C). Examination of lung pathology showed large granulomatous lesions and a decrease in the amount of free alveolar spaces that appeared to be occupied by macrophages, lymphocytes, and neutrophils in huTNF KI mice treated with anti-human TNF but not in WT mice (Fig. 5D to H). Assessment of liver pathology depicted lower numbers of granulomas in BCG-infected huTNF KI mice than WT mice when the mice were injected with NaCl. Infliximab treatment of WT mice did not change the liver granuloma pattern; however, huTNF KI mouse liver and spleen granulomas appeared to be more diffuse after infliximab treatment and presented cell death (see Fig. S5 in the supplemental material). Thus, expression of human TNF confers susceptibility to anti-human TNF-induced impaired control of BCG infection.

**HuTNF KI mice are able to control virulent *M. tuberculosis* infection, while TNF blockers render these mice susceptible.** We then asked whether huTNF KI mice were able to control a virulent *M. tuberculosis* infection. HuTNF KI, TNF KO, and WT mice were infected with *M. tuberculosis* H37Rv (1,000 CFU). TNF KO mice were highly susceptible to *M. tuberculosis* challenge, resulting in rapid weight loss after 3 weeks and death within 4 weeks, while WT mice survived the infection. Mice expressing human TNF were able to contain the infection without an appreciable body weight loss (Fig. 6A) and survived for the 2 months of the experiment (Fig. 6B) and beyond (follow-up up to 3 months; data not shown). Additionally, TNF KO mice failed to control pulmonary mycobacterial replication within the first 4 weeks of infection and developed bacterial titers 2 $\log_{10}$ units higher than those in WT mice, while the mycobacterial burden in huTNF KI mice was controlled at levels similar to those observed in WT mice (Fig. 6C). An increase in relative lung weight was a first indication of overall lung inflammation that correlated with the bacillary burden (Fig. 6D). Macroscopic examination of the lung showed no difference between WT and huTNF KI mice (Fig. 6E). Histological assessment of huTNF KI mice documented well-organized pulmonary granulomas, characterized by the accumulation of macrophages and lymphocytes, in part with perivascular and peribronchiolar lymphocyte cuffing and without necrotic area, the pulmonary granulomas appearing better structured than in WT mice. In contrast, TNF KO mice displayed massive mononuclear and neutrophil infiltration with extensive necrosis and edema without typical granulomas (Fig. 6F). In line with the high bacterial counts, ZN staining of infected lung tissue of TNF KO mice revealed abundant mycobacteria in necrotic areas, while only a few scattered mycobacteria were observed in the lungs of huTNF KI or WT mice (Fig. 6G). The amount of free alveolar space and the histological scores confirmed that the lung pathology of huTNF KI mice appeared to be similar to that of WT mice (Fig. 6H and I). Thus, the expression of human TNF is sufficient for the host to control *M. tuberculosis* infection.

Three clinically used TNF blockers were compared side-by-side in huTNF KI mice infected with *M. tuberculosis* (500 CFU, aerosol infection). Thereby, infected huTNF KI mice were treated with either infliximab, etanercept, or adalimumab starting at 2 weeks postinfection for 2 weeks. Histological assessment of infected lung tissue at 4 weeks of infection revealed that all three drugs affected granuloma integrity, characterized by massive and disorganized cellular infiltrations with large necrotic areas and eruption into bronchi. ZN staining for acid-fast bacilli revealed that the granulomas of anti-TNF-treated mice contained an overwhelming number of mycobacteria (Fig. 7A). Regarding the overall extent and quality of the lung pathology, no major differences between the three different anti-TNF regimens were observed at the doses used, although huTNF KI mice treated with etanercept appeared to have developed somewhat smaller lesions. Lung bacterial burden was also evaluated and was more than 100-fold higher following treatment with either one of the three reagents than in the mock-treated controls (Fig. 7B). Thus, during primary infection, treatment with any one of the TNF-targeted reagents was equally detrimental, resulting in uncontrolled replication of mycobacteria and disorganized granuloma formation. These data confirm that huTNF KI mice allow evaluation of human TNF-neutralizing agents in terms of their detrimental effect on host defense mechanisms against mycobacterial infections.

## DISCUSSION

Our data demonstrate that human TNF can replace mouse TNF in its capacity to efficiently induce host immunity against BCG and *M. tuberculosis* infections in mice. This study also shows that *in vitro* macrophages from huTNF KI mice respond to infectious and inflammatory stimuli as well as macrophages from WT mice by secreting cytokines and chemokines and by activating intracellular signaling. *In vivo* huTNF KI mice survived mycobacterial infections and developed Th1-type immune responses and host defense mechanisms to control the infection. During BCG infection, we noticed a delay in liver granuloma formation and IFN-γ responses in huTNF KI mice compared to the times of liver granuloma formation and the IFN-γ response in WT mice, but this was compensated for, as evidenced by regulated responses overcoming the infection. Based on these results, we conclude that human TNF in these mice is sufficient for the control of mycobacterial infections. In addition, huTNF KI mice treated with anti-human

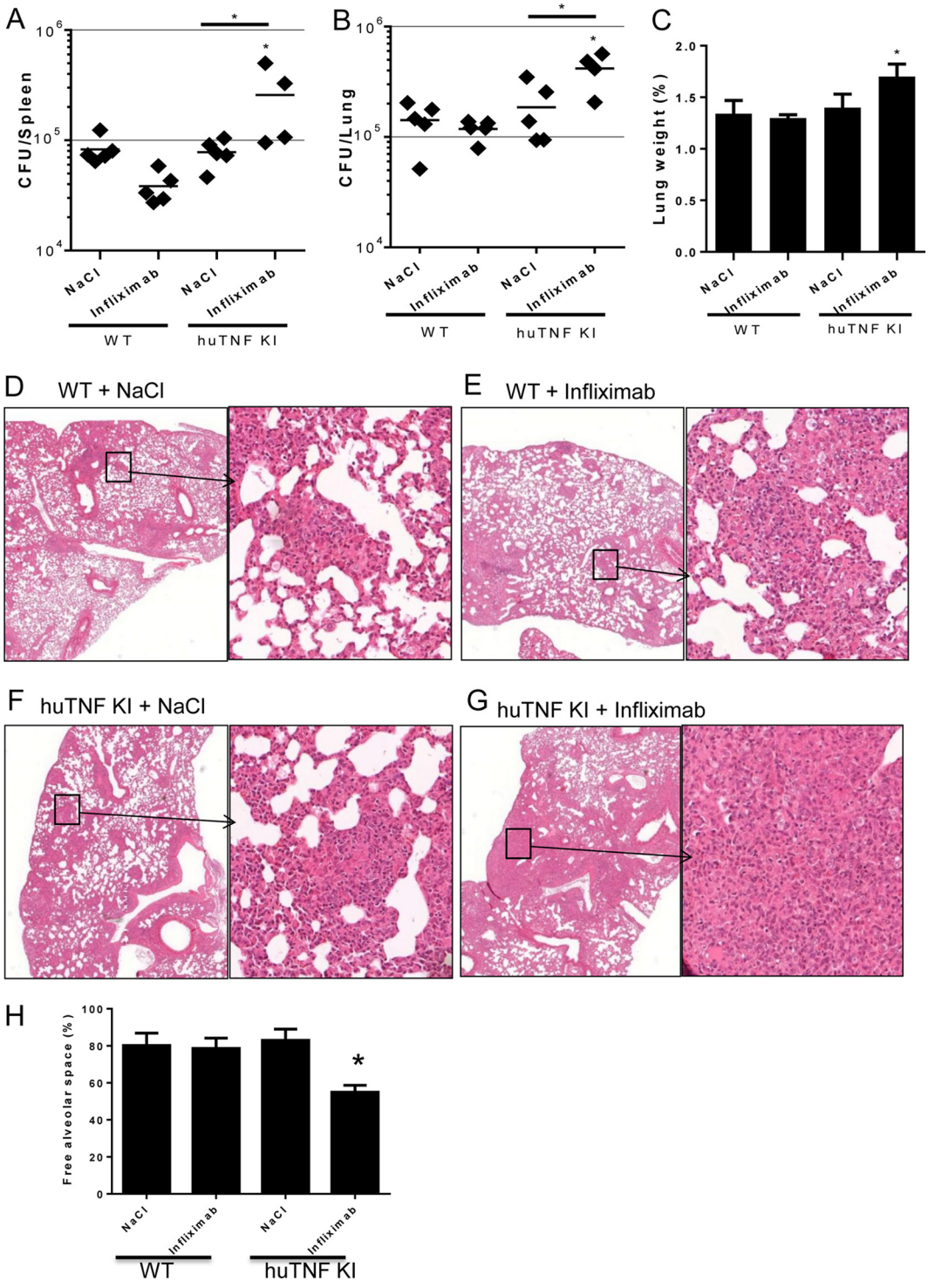


**FIG 5** HuTNF KI mice become sensitive to BCG infection upon infliximab treatment. (A and B) Bacterial loads in the spleens (A) and lungs (B) of WT and huTNF KI animals treated with infliximab or the NaCl vehicle (at day 6 of infection and twice a week thereafter) after 4 weeks of BCG Pasteur infection (i.v., $5 \times 10^6$ CFU) ($n = 5$ mice per group). The results are representative of those from five independent experiments. (C) Relative lung weights of BCG-infected mice at 4 weeks postinfection. (D to G) Microscopic examination (H&E staining) of lungs from vehicle-treated or infliximab-treated WT (D and E) and huTNF KI (F and G) mice at 4 weeks postinfection. The results are representative of those from two independent experiments. Magnifications, ×20 (left) and ×200 (right). (H) Percentage of free alveolar space in lungs from vehicle-treated and infliximab-treated WT and huTNF KI mice at 4 weeks postinfection ($n = 5$ mice per group). Bar graphs show mean ± SEM. *, $P < 0.05$ versus WT.

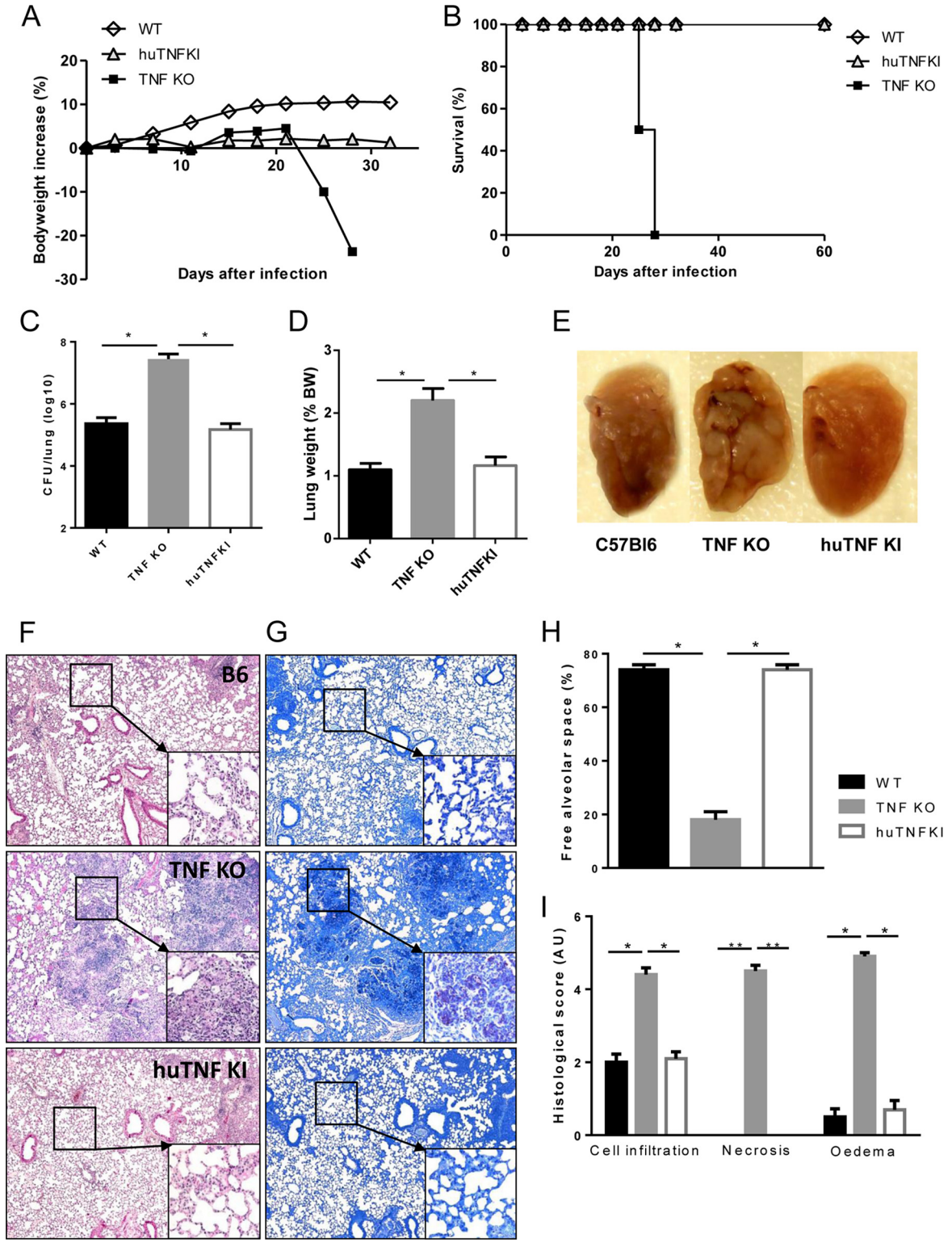


**FIG 6** Human TNF sustains host control of acute *M. tuberculosis* infection in huTNF KI mice. (A and B) WT, TNF KO, and huTNF KI mice were infected with *M. tuberculosis* H37Rv (i.n., 1,000 CFU per lung) and their body weights (A) ($n = 19$ for WT mice, $n = 22$ for huTNF KI mice, $n = 5$ for TNF KO mice) and survival (B) ($n = 8$ to 10) were monitored. Data are mean values from one experiment and are representative of those from two independent experiments. (C and D) Pulmonary bacterial loads (numbers of CFU) (C) and lung weights (D) in WT, huTNF KI, and TNF KO animals were measured at 4 weeks postinfection ($n =$ 5 mice per group). BW, body weight. (E) Macroscopic examination of infected lungs. (F and G) Microscopic examination of WT, huTNF KI, and TNF KO mice on day 28 after infection using H&E staining (F) or Ziehl-Neelsen staining (G). Magnifications, ×50, ×200 (insets in panel F), and ×400 (insets in panel G). (H and I) Semiquantitative scores of inflammatory cell infiltration into the lung, necrosis, and edema on day 28 ($n = 5$/group). Bar graphs show means ± SEMs. AU, arbitrary units. *, $P < 0.05$ versus WT; **, $P < 0.01$ versus WT.

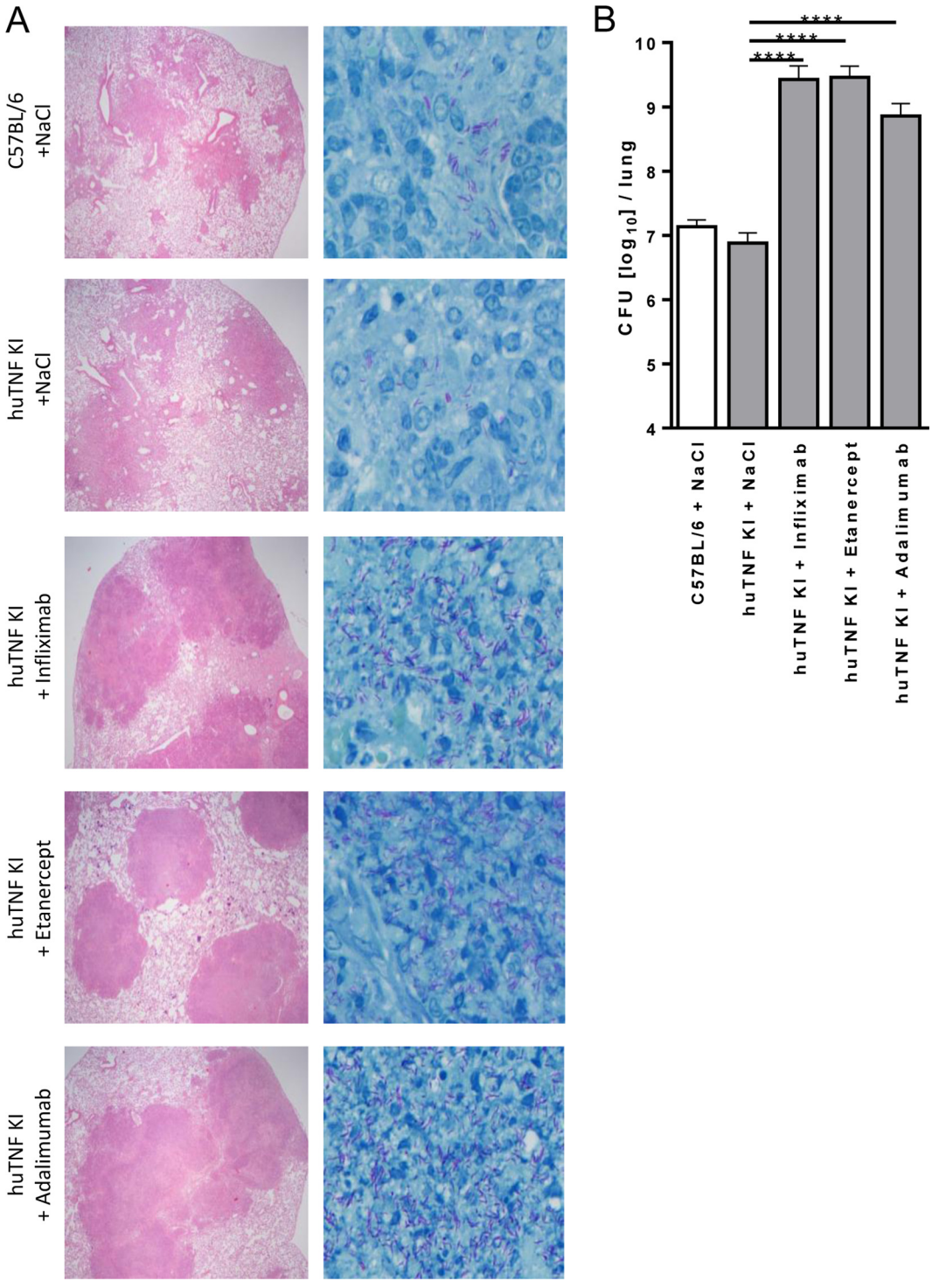


**FIG 7** Validation of the use of huTNF KI mice for evaluation and comparison of the activities of anti-human TNF compounds in *M. tuberculosis*-infected mice. (A) Lung pathology in WT, huTNF KI, and TNF-depleted huTNF KI mice treated with infliximab (10 mg/kg once a week), etanercept (40 mg/kg twice a week), and adalimumab (10 mg/kg once a week) after aerosol infection with *M. tuberculosis*. Sections obtained from diluent (NaCl)-treated and anti-TNF-treated mice at 4 weeks postinfection were stained with H&E (left) to compare the quantity and quality of granuloma formation or by the Ziehl-Neelsen method for acid-fast bacilli (right). Magnifications, ×40 (left) and ×400 (right). (B) Bacterial burden in the lungs of WT, huTNF KI, and huTNF KI mice treated with three anti-huTNF reagents at 4 weeks after aerosol infection with *M. tuberculosis* ($n = 4$ to 6 per group). Bar graphs show means ± SDs. Log-transformed data were statistically analyzed using one-way ANOVA and Bonferroni's *post hoc* test. ****, $P < 0.0001$ versus the vehicle-treated huTNFKI group.

TNF antibodies used in the clinic became sensitive to mycobacterial infections, validating the use of this animal model for testing the potential adverse effects of new specific anti-human TNF-interacting molecules.

Human TNF is known to interact with mouse TNFR1, which mediates Th1 immune responses and controls TB infection (36). This study shows that cells from huTNF KI mice activate intracellular signaling through TNFR1 similarly to WT cells. In addition, the release of TNFR1 and TNFR2 after several stimuli was comparable in huTNF KI and WT macrophages. TNFR2 has previously been shown to interact preferentially with transmembrane TNF, which plays a protective role during acute TB infection in the absence of released TNF (37). TNFR2 has been shown to play a minor role during BCG infection (38), but the upregulation and release of TNFR2 during *M. avium* infection were proposed to modulate TNF antibacterial activities (39). *M. tuberculosis*-induced release of TNFR2-neutralizing TNF was proposed to be a mechanism of evasion (40). Recently, TNFR2 has been considered to play a detrimental role via TNF neutralization by sTNFR2 during TB, with the complete absence of TNFR2 leading to the increased control of bacterial infection and survival (41).

Anti-TNF therapy for the treatment of inflammatory disease is efficient, demonstrating the critical role of TNF in the development of proinflammatory cascades sustaining chronic autoimmune inflammatory diseases. However, its inhibition has detrimental side effects that can be related to TNF activity in immune homeostasis and in host defense mechanisms (3). A critical role of TNF and TNFR1 in granuloma integrity and in the control of mycobacterial growth has been shown (42). The two types of clinically used TNF-neutralizing biologics, antibodies and sTNFR, showed distinct effects during infection, underscoring the different risks of TB reactivation. To explain these differential effects, several mouse models comparing anti-mouse TNF antibodies and murine sTNFR2 have been reported (19). In addition, computational models have been developed, and effects have been attributed to different binding kinetics and different levels of permeation of the two drugs (15, 18). However, a complete mechanistic explanation for such differences is still lacking. Our results reveal no differential effect on the overall failure to contain TB following treatment with three different anti-TNF reagents. They are proof of principle that efficient TNF neutralization is detrimental for TB control but provide no evidence that any one of the reagents is superior in terms of reducing the risk of TB reactivation. In future experiments, huTNF KI mice may be used to elucidate potential differences in the underlying molecular mechanisms of TNF neutralization by different reagents, particularly when other routes and times of administration as well as dose titration experiments with novel TNF-targeting drugs are performed. In addition, the development of next-generation human TNF blockers may now include testing in an animal model in which the animals express only human TNF to study both the therapeutic effects and the side effects of the drugs.

In conclusion, huTNF KI mice represent a useful animal model system allowing comparative evaluation of whether various species-specific human TNF-neutralizing drugs compromise host defense functions. Such effects constitute a clinically important danger of systemic anti-TNF therapy. This novel animal model with humanized TNF will be helpful for predicting the risk of TNF blocking biologics to reactivate tuberculosis infection in patients.

## ACKNOWLEDGMENTS

We thank S. Rose, R. Vacher, and C. Gabay for their various contributions throughout the project.

This work was supported by the FNS (310033_146833)(to I.G.); the joint Swiss-Russian Cooperation Program (to I.G. and S.A.N.); Ligue Pulmonaire Genevoise (to I.G.); EU FP7 grant TB-REACT (to V.F.J.Q., B.R., S.A.N., and I.G.); Region Centre France (to V.F.J.Q. and B.R.); a special grant from Wyeth (to S.E. and S.A.N.); a BMBF grant, TTU Tuberculosis: German Center for Infection Research (to S.E. and K.W.); RFBR (13-04-02052) (to M.S.D.); the Ministry of Education and Science of Russian Federation (contract no. 14.Z50.31.0008) (to S.A.N.); the Fondation Ernst et Lucie Schmidheiny (to M.L.O.); and the Consejo Nacional de Ciencia y Tecnología (CONACyT), México (fellowship 207760 to L.C.-G.).

## REFERENCES

1. **Aggarwal BB, Gupta SC, Kim JH.** 2012. Historical perspectives on tumor necrosis factor and its superfamily: 25 years later, a golden journey. Blood **119:**651–665. http://dx.doi.org/10.1182/blood-2011-04-325225.
2. **Kruglov AA, Kuchmiy A, Grivennikov SI, Tumanov AV, Kuprash DV, Nedospasov SA.** 2008. Physiological functions of tumor necrosis factor and the consequences of its pathologic overexpression or blockade: mouse models. Cytokine Growth Factor Rev **19:**231–244. http://dx.doi.org/10.1016/j.cytogfr.2008.04.010.
3. **Vassalli P.** 1992. The pathophysiology of tumor necrosis factors. Annu Rev Immunol **10:**411–452. http://dx.doi.org/10.1146/annurev.iy.10.040192.002211.
4. **Kollias G, Douni E, Kassiotis G, Kontoyiannis D.** 1999. On the role of tumor necrosis factor and receptors in models of multiorgan failure, rheumatoid arthritis, multiple sclerosis and inflammatory bowel disease. Immunol Rev **169:**175–194. http://dx.doi.org/10.1111/j.1600-065X.1999.tb01315.x.
5. **Garcia I, Olleros ML, Quesniaux VF, Jacobs M, Allie N, Nedospasov SA, Szymkowski DE, Ryffel B.** 2011. Roles of soluble and membrane TNF and related ligands in mycobacterial infections: effects of selective and non-selective TNF inhibitors during infection. Adv Exp Med Biol **691:**187–201. http://dx.doi.org/10.1007/978-1-4419-6612-4_20.
6. **Tracey D, Klareskog L, Sasso EH, Salfeld JG, Tak PP.** 2008. Tumor necrosis factor antagonist mechanisms of action: a comprehensive review. Pharmacol Ther **117:**244–279. http://dx.doi.org/10.1016/j.pharmthera.2007.10.001.
7. **Rennard SI, Flavin SK, Agarwal PK, Lo KH, Barnathan ES.** 2013. Long-term safety study of infliximab in moderate-to-severe chronic obstructive pulmonary disease. Respir Med **107:**424–432. http://dx.doi.org/10.1016/j.rmed.2012.11.008.
8. **Rennard SI, Fogarty C, Kelsen S, Long W, Ramsdell J, Allison J, Mahler D, Saadeh C, Siler T, Snell P, Korenblat P, Smith W, Kaye M, Mandel M, Andrews C, Prabhu R, Donohue JF, Watt R, Lo KH, Schlenker-Herceg R, Barnathan ES, Murray J, COPD Investigators.** 2007. The safety and efficacy of infliximab in moderate to severe chronic obstructive pulmonary disease. Am J Respir Crit Care Med **175:**926–934. http://dx.doi.org/10.1164/rccm.200607-995OC.
9. **Keane J.** 2005. TNF-blocking agents and tuberculosis: new drugs illuminate an old topic. Rheumatology (Oxford) **44:**714–720. http://dx.doi.org/10.1093/rheumatology/keh567.
10. **Solovic I, Sester M, Gomez-Reino JJ, Rieder HL, Ehlers S, Milburn HJ, Kampmann B, Hellmich B, Groves R, Schreiber S, Wallis RS, Sotgiu G, Scholvinck EH, Goletti D, Zellweger JP, Diel R, Carmona L, Bartalesi F, Ravn P, Bossink A, Duarte R, Erkens C, Clark J, Migliori GB, Lange C.** 2010. The risk of tuberculosis related to tumour necrosis factor antagonist therapies: a TBNET consensus statement. Eur Respir J **36:**1185–1206. http://dx.doi.org/10.1183/09031936.00028510.
11. **Wallis RS.** 2008. Tumour necrosis factor antagonists: structure, function, and tuberculosis risks. Lancet Infect Dis **8:**601–611. http://dx.doi.org/10.1016/S1473-3099(08)70227-5.
12. **Yoo JW, Jo KW, Kang BH, Kim MY, Yoo B, Lee CK, Kim YG, Yang SK, Byeon JS, Kim KJ, Ye BD, Shim TS.** 2014. Mycobacterial diseases developed during anti-tumour necrosis factor-alpha therapy. Eur Respir J **44:**1289–1295. http://dx.doi.org/10.1183/09031936.00063514.
13. **Dye C, Fine PE.** 2013. A major event for new tuberculosis vaccines. Lancet **381:**972–974. http://dx.doi.org/10.1016/S0140-6736(13)60137-3.

14. **Dye C, Glaziou P, Floyd K, Raviglione M.** 2013. Prospects for tuberculosis elimination. Annu Rev Public Health **34:**271–286. http://dx.doi.org/10.1146/annurev-publhealth-031912-114431.
15. **Wallis RS, Ehlers S.** 2005. Tumor necrosis factor and granuloma biology: explaining the differential infection risk of etanercept and infliximab. Semin Arthritis Rheum **34:**34–38. http://dx.doi.org/10.1016/j.semarthrit.2005.01.009.
16. **Wallis RS.** 2009. Infectious complications of tumor necrosis factor blockade. Curr Opin Infect Dis **22:**403–409. http://dx.doi.org/10.1097/QCO.0b013e32832dda55.
17. **Marino S, Sud D, Plessner H, Lin PL, Chan J, Flynn JL, Kirschner DE.** 2007. Differences in reactivation of tuberculosis induced from anti-TNF treatments are based on bioavailability in granulomatous tissue. PLoS Comput Biol **3:**1909–1924.
18. **Fallahi-Sichani M, Flynn JL, Linderman JJ, Kirschner DE.** 2012. Differential risk of tuberculosis reactivation among anti-TNF therapies is due to drug binding kinetics and permeability. J Immunol **188:**3169–3178. http://dx.doi.org/10.4049/jimmunol.1103298.
19. **Plessner HL, Lin PL, Kohno T, Louie JS, Kirschner D, Chan J, Flynn JL.** 2007. Neutralization of tumor necrosis factor (TNF) by antibody but not TNF receptor fusion molecule exacerbates chronic murine tuberculosis. J Infect Dis **195:**1643–1650. http://dx.doi.org/10.1086/517519.
20. **Winsauer C, Kruglov AA, Chashchina AA, Drutskaya MS, Nedospasov SA.** 2014. Cellular sources of pathogenic and protective TNF and experimental strategies based on utilization of TNF humanized mice. Cytokine Growth Factor Rev **25:**115–123. http://dx.doi.org/10.1016/j.cytogfr.2013.12.005.
21. **Marino MW, Dunn A, Grail D, Inglese M, Noguchi Y, Richards E, Jungbluth A, Wada H, Moore M, Williamson B, Basu S, Old LJ.** 1997. Characterization of tumor necrosis factor-deficient mice. Proc Natl Acad Sci U S A **94:**8093–8098. http://dx.doi.org/10.1073/pnas.94.15.8093.
22. **Fotio AL, Olleros ML, Vesin D, Tauzin S, Bisig R, Dimo T, Nguelefack TB, Dongo E, Kamtchouing P, Garcia I.** 2010. In vitro inhibition of lipopolysaccharide and Mycobacterium bovis bacillus Calmette Guerin-induced inflammatory cytokines and in vivo protection from D-galactosamine/LPS-mediated liver injury by the medicinal plant Sclerocarya birrea. Int J Immunopathol Pharmacol **23:**61–72.
23. **Olleros ML, Vesin D, Lambou AF, Janssens JP, Ryffel B, Rose S, Fremond C, Quesniaux VF, Szymkowski DE, Garcia I.** 2009. Dominant-negative tumor necrosis factor protects from Mycobacterium bovis bacillus Calmette Guerin (BCG) and endotoxin-induced liver injury without compromising host immunity to BCG and Mycobacterium tuberculosis. J Infect Dis **199:**1053–1063. http://dx.doi.org/10.1086/597204.
24. **Garcia I, Miyazaki Y, Araki K, Araki M, Lucas R, Grau GE, Milon G, Belkaid Y, Montixi C, Lesslauer W, Vassalli P.** 1995. Transgenic mice expressing high levels of soluble TNF-R1 fusion protein are protected from lethal septic shock and cerebral malaria, and are highly sensitive to Listeria monocytogenes and Leishmania major infections. Eur J Immunol **25:**2401–2407. http://dx.doi.org/10.1002/eji.1830250841.
25. **Stefanova T, Chouchkova M, Hinds J, Butcher PD, Inwald J, Dale J, Palmer S, Hewinson RG, Gordon SV.** 2003. Genetic composition of Mycobacterium bovis BCG substrain Sofia. J Clin Microbiol **41:**5349. http://dx.doi.org/10.1128/JCM.41.11.5349.2003.
26. **Olleros ML, Vesin D, Bisig R, Santiago-Raber ML, Schuepbach-Mallepell S, Kollias G, Gaide O, Garcia I.** 2012. Membrane-bound TNF induces protective immune responses to M. bovis BCG infection: regulation of memTNF and TNF receptors comparing two memTNF molecules. PLoS One **7:**e31469. http://dx.doi.org/10.1371/journal.pone.0031469.
27. **Allie N, Keeton R, Court N, Abel B, Fick L, Vasseur V, Vacher R, Olleros ML, Drutskaya MS, Guler R, Nedospasov SA, Garcia I, Ryffel B, Quesniaux VF, Jacobs M.** 2010. Limited role for lymphotoxin α in the host immune response to Mycobacterium tuberculosis. J Immunol **185:**4292–4301. http://dx.doi.org/10.4049/jimmunol.1000650.
28. **Ehlers S, Holscher C, Scheu S, Tertilt C, Hehlgans T, Suwinski J, Endres R, Pfeffer K.** 2003. The lymphotoxin beta receptor is critically involved in controlling infections with the intracellular pathogens Mycobacterium tuberculosis and Listeria monocytogenes. J Immunol **170:**5210–5218. http://dx.doi.org/10.4049/jimmunol.170.10.5210.
29. **Guler R, Olleros ML, Vesin D, Parapanov R, Garcia I.** 2005. Differential effects of total and partial neutralization of tumor necrosis factor on cell-mediated immunity to Mycobacterium bovis BCG infection. Infect Immun **73:**3668–3676. http://dx.doi.org/10.1128/IAI.73.6.3668-3676.2005.
30. **Segueni N, Vigne S, Palmer G, Bourigault ML, Olleros ML, Vesin D, Garcia I, Ryffel B, Quesniaux VF, Gabay C.** 2015. Limited contribution of IL-36 versus IL-1 and TNF pathways in host response to mycobacterial infection. PLoS One **10:**e0126058. http://dx.doi.org/10.1371/journal.pone.0126058.
31. **Olleros ML, Vesin D, Fotio AL, Santiago-Raber ML, Tauzin S, Szymkowski DE, Garcia I.** 2010. Soluble TNF, but not membrane TNF, is critical in LPS-induced hepatitis. J Hepatol **53:**1059–1068. http://dx.doi.org/10.1016/j.jhep.2010.05.029.
32. **Olleros ML, Guler R, Corazza N, Vesin D, Eugster HP, Marchal G, Chavarot P, Mueller C, Garcia I.** 2002. Transmembrane TNF induces an efficient cell-mediated immunity and resistance to Mycobacterium bovis bacillus Calmette-Guerin infection in the absence of secreted TNF and lymphotoxin-alpha. J Immunol **168:**3394–3401. http://dx.doi.org/10.4049/jimmunol.168.7.3394.
33. **Garcia I, Miyazaki Y, Marchal G, Lesslauer W, Vassalli P.** 1997. High sensitivity of transgenic mice expressing soluble TNFR1 fusion protein to mycobacterial infections: synergistic action of TNF and IFN-gamma in the differentiation of protective granulomas. Eur J Immunol **27:**3182–3190. http://dx.doi.org/10.1002/eji.1830271215.
34. **Garcia I, Guler R, Vesin D, Olleros ML, Vassalli P, Chvatchko Y, Jacobs M, Ryffel B.** 2000. Lethal Mycobacterium bovis bacillus Calmette Guerin infection in nitric oxide synthase 2-deficient mice: cell-mediated immunity requires nitric oxide synthase 2. Lab Invest **80:**1385–1397. http://dx.doi.org/10.1038/labinvest.3780146.
35. **Kindler V, Sappino AP, Grau GE, Piguet PF, Vassalli P.** 1989. The inducing role of tumor necrosis factor in the development of bactericidal granulomas during BCG infection. Cell **56:**731–740. http://dx.doi.org/10.1016/0092-8674(89)90676-4.
36. **Flynn JL, Goldstein MM, Chan J, Triebold KJ, Pfeffer K, Lowenstein CJ, Schreiber R, Mak TW, Bloom BR.** 1995. Tumor necrosis factor-alpha is required in the protective immune response against Mycobacterium tuberculosis in mice. Immunity **2:**561–572. http://dx.doi.org/10.1016/1074-7613(95)90001-2.
37. **Dambuza I, Allie N, Fick L, Johnston N, Fremond C, Mitchell J, Quesniaux VF, Ryffel B, Jacobs M.** 2008. Efficacy of membrane TNF mediated host resistance is dependent on mycobacterial virulence. Tuberculosis (Edinb) **88:**221–234. http://dx.doi.org/10.1016/j.tube.2007.08.011.
38. **Jacobs M, Brown N, Allie N, Chetty K, Ryffel B.** 2000. Tumor necrosis factor receptor 2 plays a minor role for mycobacterial immunity. Pathobiology **68:**68–75. http://dx.doi.org/10.1159/000028116.
39. **Corti A, Fattorini L, Thoresen OF, Ricci ML, Gallizia A, Pelagi M, Li Y, Orefici G.** 1999. Upregulation of p75 tumor necrosis factor alpha receptor in Mycobacterium avium-infected mice: evidence for a functional role. Infect Immun **67:**5762–5767.
40. **Balcewicz-Sablinska MK, Keane J, Kornfeld H, Remold HG.** 1998. Pathogenic Mycobacterium tuberculosis evades apoptosis of host macrophages by release of TNF-R2, resulting in inactivation of TNF-alpha. J Immunol **161:**2636–2641.
41. **Keeton R, Allie N, Dambuza I, Abel B, Hsu NJ, Sebesho B, Randall P, Burger P, Fick E, Quesniaux VF, Ryffel B, Jacobs M.** 2014. Soluble TNFRp75 regulates host protective immunity against Mycobacterium tuberculosis. J Clin Invest **124:**1537–1551. http://dx.doi.org/10.1172/JCI45005.
42. **Fallahi-Sichani M, El-Kebir M, Marino S, Kirschner DE, Linderman JJ.** 2011. Multiscale computational modeling reveals a critical role for TNF-alpha receptor 1 dynamics in tuberculosis granuloma formation. J Immunol **186:**3472–3483. http://dx.doi.org/10.4049/jimmunol.1003299.